PHYSICAL REVIEW D VOLUME 25, NUMBER 1 1 JANUARY 1982

Angular distributions of high-mass dileptons in high-energy hadronic collisions

M. Chaichian
Department of High Energy Physics, University of Helsinki, Helsinki, Finland

M. Hayashi
Department of Physics, Saitama Medical College, Moroyama, Saitama, 350-04 Japan

K. Yamagishi
Department of Physics, Tokuyama University, Yamaguchi, 745 Japan
(Received 8 June 1981)

The angular distrubutions for dileptons arising from decays of a virtual photon and the Z^0 produced in hadronic collisions are calculated at large mass and finite transverse momentum of dileptons in the lowest order of quantum chromodynamics and the Weinberg-Salam model with threee fermion generations. Numerical evaluation for coefficients of the distributions is carried out for $\bar{p}p$ collisions at $\sqrt{s}=540$ GeV and pp at $\sqrt{s}=800$ GeV in different (helicity, Gottfried-Jackson, and Collins-Soper) reference frames. Coefficients of parity-violating terms in the distributions exhibit clean signs of the Z^0 boson, while those of parity-conserving terms are quite insensitive to the presence of the Z^0 boson.

I. INTRODUCTION

The electroweak theory of Weinberg and Salam has been successful in explaining many aspects of present experimental facts. Yet direct observation of the intermediate vector bosons is necessary to study various problems, such as the neutral weak current, the Higgs mechanism, and the number of fermion generations.[1] It was pointed out that production of lepton pairs in hadron-hadron collisions provides us with an excellent laboratory for their detection and investigation.[2] On the other hand, it is widely recognized that angular distributions of leptons involve important information about the production mechanism of the lepton pairs.[3-9]

In this paper we will calculate the angular distributions of lepton pairs, at large mass M and finite transverse momentum Q_T, arising from decays of a virtual photon γ^* and Z^0 boson formed in high-energy hadronic collisions.

$$\text{hadron (beam)}+\text{hadron (target)} \rightarrow (\gamma^*, Z^0)+X \searrow l^+l^- \quad (l=e \text{ or } \mu)\,, \tag{1.1}$$

using the lowest order of quantum chromodynamics (QCD).

As is known the Drell-Yan process via γ^* predicts $1+\cos^2\theta$ distribution at $Q_T=0$, where θ is a lepton-pair angle in its rest system.[3,10] For small values of Q_T, intrinsic transverse momentum of partons in colliding hadrons smears this simple distribution,[4] although such smearing can be very small for large M^2. For large M^2 and finite Q_T, where the zeroth order of the Drell-Yan process gives no contribution and the effect of the intrinsic transverse momentum is suppressed, the first-order processes in α_s, such as the annihilation process in which a quark (q) and an antiquark ($\bar{q}$) annihilate into a heavy boson (γ^* or Z^0) and a gluon (G) and its crossed Compton process, dominate and give angular distributions other than the simple $1+\cos^2\theta$. At large M^2 and finite Q_T the running coupling constant α_s of QCD is small and results calculated in this way are infrared insenitive.[11] This means that the lowest-order calculation in α_s is reliable and safe to compare with experimental data.

Discussions of the lepton angular distributions given by several authors are concerned mostly with QCD tests.[5-9] They took into account only pro-

cessess of a virtual photon γ^* decaying into two leptons. In this paper we focus our attention on the lepton angular distributions, where the Z^0 boson also gives contributions in addition to γ^*. We have calculated subprocesses $q+\bar{q}\rightarrow(\gamma^*$ or $Z^0)+G$ and $q+G\rightarrow(\gamma^*$ or $Z^0)+q$ at large M and finite Q_T. For the interactions between the Z^0 boson and the fermions we assume the standard SU(2)×U(1) Weinberg-Salam model, with quarks and leptons in three generations, i.e., six flavors.

The angular distribution we have obtained can be written, in terms of angles θ and φ of a lepton in the lepton-pair rest system, as

$$D(A_0,A_1,A_2,A_3,A_4)=1+\cos^2\theta+A_0(\tfrac{1}{2}-\tfrac{3}{2}\cos^2\theta)+A_1\sin 2\theta\cos\varphi +A_2\tfrac{1}{2}\sin^2\theta\cos 2\varphi+A_3\sin\theta\cos\varphi+A_4\cos\varphi\ , \tag{1.2}$$

where the A_i's ($i=0,1,2,3,4$) are functions of the total c.m. energy $\sqrt{s}$ and M^2, Q_T, and rapidity y of the lepton pair. Coefficients of parity-violating terms A_3 and A_4 come from contributions of the axial-vector neutral currents, while A_0, A_1, and A_2 are parity-conserving coefficients arising from the neutral and electromagnetic currents. We have evaluated these coefficients in three frames, i.e., the s-channel helicity (H) frame, the Gottfried-Jackson (GJ) frame, and the Collins-Soper (CS) frame,[4] for high-energy $\bar{p}p$ and pp collisions. We have found that the parity-conserving coefficients are not suitable for the study of the Z^0, but A_3 and A_4 provide clear effects of the Z^0 boson.

In Sec. II, we derive the lepton angular distribution in high-energy hadron-hadron collisions by calculating the first-order diagrams of QCD. Numerical evaluation of the coefficients in the angular distribution for $\bar{p}p$ and pp collisions is carried out in Sec. III, employing the Glück-Owens-Reya parametrization[12] for the parton distributions. We have plotted the coefficients at energy $\sqrt{s}=540$ GeV for $\bar{p}p$ and at $\sqrt{s}=800$ GeV for pp, which will be experimentally feasible in the near future, as functions of either $\sqrt{\tau}=M/\sqrt{s}$ or $r=Q_T/M$. Section IV is devoted to the conclusions.

II. ANGULAR DISTRIBUTION OF THE LEPTON PAIR IN HADRONIC COLLISIONS

In this section we derive the angular distribution of lepton pairs produced in high-energy hadronic collisions. Since we are interested in the Z^0 production we restrict ourselves to a kinematical region of high-mass dileptons.

At finite transverse momenta of the dilepton, the angular distributions are dominated, within the framework of QCD, by diagrams of Fig. 1. There are two contributions: diagrams (a) give the quark-antiquark annihilation contribution, and diagrams (b) the quark-gluon Comton scattering contribuition.

A. Quark-antiquark annihilation

The differential cross section of lepton pair production for collisions of hardons with initial incident (beam) momentum P^B and a target momentum P^T is constructed by convoluting the cross section of the subprocess of partons with momenta $p_1=x_1P^B$ and $p_2=x_2P^T$ with the parton distributions.

Let us denote by f_i^B a distribution function of quark i in the incident hadron and by $f_{\bar{i}}^T$ that of the antiquark $\bar{i}$ in the target hadron etc., and write the parton differential cross section at fixed M, and $\hat{t}=(Q-p_1)^2$, and a solid angle $\Omega_1^*=(\theta,\varphi)$ of one of the leptons in the dilepton system as $d\hat{\sigma}_A/dM^2d\hat{t}\times d\Omega_1^*$ (caret denotes quantities at the parton level). Then the hadronic differential cross section of the lepton pair from the decays of the γ^* and Z^0 at fixed M^2, Q_T, y, and solid angle Ω_1^* and of a jet at fixed rapidity y_j is given by[5]

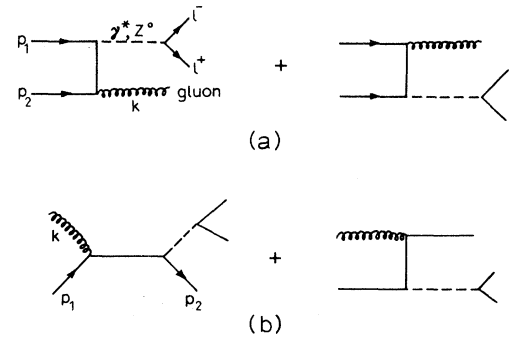

FIG. 1. (a) The quark-antiquark annihilation diagrams. (b) The quark-gluon Compton diagrams.

$$\frac{d\sigma_A}{dM^2dy\,dQ_T{}^2dy_jd\Omega_1^*}=\sum_i x_1x_2\left[f_i^B(x_1)f_{\bar{i}}^T(x_2)\frac{d\hat{\sigma}_A}{dM^2d\hat{t}\,d\Omega_1^*}+(i\leftrightarrow\bar{i})\right], \tag{2.1}$$

where (and hereafter) the summation should be carried out for all relevant quark flavors $i=u,d,s,\ldots$ but not for their antiparticle states $\bar{u},\bar{d},\bar{s}\ldots$, and A stands for the annihilation.

The parton cross section, giving the angular distribution for one of the leptons (hereafter, for definiteness, we take $l^-=e^-$ or μ^-; the corresponding angular distribution for $l^+=e^+$ or μ^+ is obtained by replacing $L_i\rightarrow -L_i$, $K_i\rightarrow K_i$ in the following equations), can be easily calculated for massless quarks and is written as a product of the differential cross section integrated over the lepton angles $d\hat{\sigma}_A/dM^2d\hat{t}$ and a function of initial quark and antiquark momenta $\vec{p}_1$ and $\vec{p}_2$ in the lepton-pair c.m. system

$$\frac{d\hat{\sigma}_A}{dM^2\,d\hat{t}\,d\Omega_1^*}=\frac{d\hat{\sigma}_A}{dM^2d\hat{t}}\frac{3}{16\pi}\left[1+\frac{p_{1q}{}^2+p_{2q}{}^2}{|\vec{p}_1|^2+|\vec{p}_2|^2}+\frac{2L_i}{K_i}\frac{|\vec{p}_i|\,p_{1q}-|\vec{p}_2|\,p_{2q}}{|\vec{p}_1|^2+|\vec{p}_2|^2}\right], \tag{2.2}$$

where p_{iq} $(i=1,2)$ is a projection of $\vec{p}_i$ in the direction of the lepton momentum $\vec{q}$,

$$p_{iq}=p_{ix}\sin\theta\cos\varphi+p_{iz}\cos\theta\quad(i=1,2)\,. \tag{2.3}$$

Note that when calculating the term $(i\leftrightarrow\bar{i})$ in Eq. (2.1), one has to replace $p_1\leftrightarrow p_2$ in Eq. (2.2) [in the case of annihilation, we keep the relation: $p_1=x_1P^B$, $p_2=x_2P^T$ for the crossed term $(i\leftrightarrow\bar{i})$ as well; see Appendix A].

All information about the neutral currents is contained in K_i and L_i, and especially the term containing L_i reflects the intrinsic parity-violating nature of the Z^0.

$$\begin{aligned}K_i&=\frac{(a_i{}^2+b_i{}^2)(a^2+b^2)}{\sin^4\theta_W\cos^4\theta_W}|D_{Z^0}|^2\\&\quad-\frac{2e_iaa_i}{\sin^2\theta_W\cos^2\theta_W}\frac{\mathrm{Re}D_{Z^0}}{M^2}+\frac{e_i{}^2}{M^4}\,,\\L_i&=\frac{4aba_ib_i}{\sin^4\theta_W\cos^4\theta_W}|D_{Z^0}|^2\\&\quad-\frac{2e_ibb_i}{\sin^2\theta_W\cos^2\theta_W}\frac{\mathrm{Re}D_{Z^0}}{M^2}\,,\end{aligned} \tag{2.4}$$

where a_i and b_i (a and b) are the vector and the axial-vector coupling constants, in units of e, of the quark i (the lepton) to the Z^0 boson, e_i is the charge of the quark i divided by e, and θ_W is the Weinberg angle,

$$\begin{aligned}&b_i=\tfrac{1}{4}\text{ for }i=u,\ c,\text{ or }t,\\a_i&=-e_i\sin^2\theta_W+b_i,\\&b_i=-\tfrac{1}{4}\text{ for }i=d,\ s,\text{ or }b\,,\end{aligned} \tag{2.5}$$

$$a=\sin^2\theta_W-\tfrac{1}{4},\quad b=-\tfrac{1}{4}\text{ for }e,\ \mu,\text{ or }\tau\,,$$

$$a=\tfrac{1}{4},\quad b=\tfrac{1}{4}\text{ for }\nu_e,\ \nu_\mu,\text{ or }\nu_\tau\,,$$

and the propagator of the Z^0 with its mass M_{Z^0} and the width Γ_{Z^0} is given by

$$\begin{aligned}D_{Z^0}&=(M^2-M_{Z^0}{}^2+iM_{Z^0}\Gamma_{Z^0})^{-1}\,,\\\mathrm{Re}D_{Z^0}&=(M^2-M_{Z_0}{}^2)\,|D_{Z^0}|^2\,.\end{aligned} \tag{2.6}$$

The differential cross section $d\hat{\sigma}_A/dM^2d\hat{t}$ is given by

$$\frac{d\hat{\sigma}_A}{dM^2\,d\hat{t}}=\frac{4}{9}\times\frac{2}{3}\frac{\alpha^2\alpha_s}{\hat{s}^2}M^2\frac{T^2+U^2}{\hat{t}\hat{u}}K_i\,, \tag{2.7}$$

where $\frac{4}{9}$ is a color-averaging factor, and α being the fine-structure constant. Here kinematical variables are

$$\begin{aligned}&\hat{s}=(p_1+p_2)^2,\quad\hat{u}=(p_2-Q)^2,\quad\hat{t}=(Q-p_1)^2\,,\\&T=\hat{t}-M^2,\quad U=\hat{u}-M^2\,.\end{aligned} \tag{2.8}$$

Using Eq. (2.3) and putting Eq. (2.2) into Eq. (2.1), we obtain

$$\frac{d\sigma_A}{dM^2dy\,dQ_T{}^2dy_jd\Omega_1^*}=\frac{d\sigma_A}{dM^2\,dy\,dQ_T{}^2dy_j}\frac{3}{16\pi}D(\hat{A}_0(A),\hat{A}_1(A),\hat{A}_2(A),\xi\hat{A}_3(A),\xi\hat{A}_4(A))\,, \tag{2.9}$$

where $d\sigma_A/dM^2\,dy\,dQ_T{}^2\,dy_j$ is the hadronic differential cross-section integrated over the lepton angles

$$\frac{d\sigma_A}{dM^2dy\,dQ_T{}^2dy_j}=\sum_i x_1x_2F_i(x_1,x_2)\frac{d\hat{\sigma}_A}{dM^2\,d\hat{t}} \tag{2.10}$$

and

$$D(\hat{A}_0(A),\hat{A}_1(A),\hat{A}_2(A),\xi\hat{A}_3(A),\xi\hat{A}_4(A))=1+\cos^2\theta+\hat{A}_0(A)(\tfrac{1}{2}-\tfrac{3}{2}\cos^2\theta)$$
$$+\hat{A}_1(A)\sin 2\theta\cos\varphi+\hat{A}_2(A)\tfrac{1}{2}\sin^2\theta\cos 2\varphi$$
$$+\xi\hat{A}_3(A)\sin\theta\cos\varphi+\xi\hat{A}_4(A)\cos\theta\ , \tag{2.11}$$

with

$$\hat{A}_0(A)=\hat{A}_2(A)=\frac{p_{1x}{}^2+p_{2x}{}^2}{|\vec{p}_1|^2+|\vec{p}_2|^2},\quad \hat{A}_1(A)=\frac{p_{1x}p_{1z}+p_{2x}p_{2z}}{|\vec{p}_1|^2+|\vec{p}_2|^2}\ ,$$
$$\hat{A}_3(A)=\frac{|\vec{p}_1|p_{1x}-p_{2x}|\vec{p}_2|}{|\vec{p}_1|^2+|\vec{p}_2|^2}\ ,\quad \hat{A}_4(A)=\frac{|\vec{p}_1|p_{1z}-p_{2z}|\vec{p}_2|}{|\vec{p}_1|^2+|\vec{p}_2|^2}\ , \tag{2.12}$$
$$\xi=2\frac{\sum_i x_1x_2G_i(x_1,x_2)L_i}{\sum_i x_1x_2F_i(x_1,x_2)K_i}\ ,$$
$$F_i(x_1,x_2)=f_i^B(x_1)f_{\bar{i}}^T(x_2)+f_{\bar{i}}^B(x_1)f_i^T(x_2),\quad G_i(x_1,x_2)=f_i^B(x_1)f_{\bar{i}}^T(x_2)-f_{\bar{i}}^B(x_1)f_i^T(x_2)\ .$$

A in brackets stands for the annihilation subprocess.

Now integration over the jet rapidity y in Eq. (2.9) gives the angular distribution $D(A_0(A),A_1(A),A_2(A),A_3(A),A_4(A))$ at the hadron level at fixed M, Q_T, and y for a given energy $\sqrt{s}$. The coefficients are written as

$$A_i(A)\frac{d\sigma_A}{dM^2dy\,dQ_T{}^2}=\begin{cases}\int dy_j\dfrac{d\sigma_A}{dM^2dy\,dQ_T{}^2dy_j}\hat{A}_i(A),\quad i=0,1,2\ ,\\ \int dy_j\dfrac{d\sigma_A}{dM^2dy\,dQ_T{}^2dy_j}\xi\hat{A}_i(A),\quad i=3,4\ ,\end{cases} \tag{2.13}$$

where

$$\frac{d\sigma_A}{dM^2dy\,dQ_T{}^2}=\int dy_j\frac{d\sigma_A}{dM^2dy\,dQ_T{}^2dy_j}\ . \tag{2.14}$$

B. The gluon-quark Compton scattering

Expressions for the Compton scattering can be obtained from those for the annihilation cross section, i.e., by replacing $k\to -k$, $p_2\to -p_2$ in the corresponding formulas. In this case we have to consider two cases separately: case 1, a gluon is in the beam hadron and a quark (or antiquark) in the target hadron; case 2, a quark (or antiquark) in the beam and a gluon in the target.

The hadronic differential cross section for case 1 reads as

$$\left.\frac{d\sigma_C}{dM^2dy\,dQ_T{}^2dy_j\,d\Omega_1^*}\right|_1=\sum_i F_{1i}(x_1,x_2)x_1x_2\left.\frac{d\sigma_C}{dM^2d\hat{t}\,d\Omega_1^*}\right|_1\ , \tag{2.15}$$

where the parton cross section is given by (C stands for Compton scattering)

$$\left.\frac{d\hat{\sigma}_C}{dM^2d\hat{t}\,d\Omega_1^*}\right|_1=\frac{d\hat{\sigma}_C}{dM^2d\hat{t}}\frac{3}{16\pi}\left[1+\frac{p_{1q}{}^2+p_{2q}{}^2}{|\vec{p}_1|^2+|\vec{p}_2|^2}+\frac{2L_i}{K_i}\frac{|\vec{p}_i|p_{1q}+p_{2q}|\vec{p}_2|}{|\vec{p}_1|^2+|\vec{p}_2|^2}\right] \tag{2.16}$$

with

$$\left.\frac{d\hat{\sigma}_C}{dM^2d\hat{t}}\right|_1=\frac{1}{6}\times\frac{2}{3}\frac{\alpha^2\alpha_s}{\hat{s}^2}\frac{s^2+U^2}{-\hat{s}\hat{u}}M^2K_i \tag{2.17}$$

with $S=\hat{s}-M^2$ and $\frac{1}{6}$ being a color-averging factor and

$$F_{1i}(x_1,x_2)=f^B_{\text{gluon}}(x_1)[f_i^T(x_2)+f_{\bar{i}}^T(x_2)] \ . \tag{2.18}$$

[$f^B_{\text{gluon}}(x_1)$ denotes the distribution function of the gluon in the beam hadron, etc.] Similarly as in Eq. (2.9) we have

$$\left.\frac{d\sigma_C}{dM^2dy\,dQ_T{}^2dy_jd\Omega_1^*}\right|_1=\left.\frac{d\sigma_c}{dM^2dy\,Q_T{}^2dy_j}\right|_1\frac{3}{16\pi}D(\hat{A}_0(C),\hat{A}_1(C),\hat{A}_2(C),\xi_1\hat{A}_3(C),\xi_1\hat{A}_4(C))\,|_1 \ , \tag{2.19}$$

where

$$\left.\frac{d\sigma_C}{dM^2dy\,dQ_T{}^2dy_j}\right|_1=\sum_i F_{1i}(x_1,x_2)x_1x_2\left.\frac{d\hat{\sigma}_c}{dM^2\,d\hat{t}}\right|_1 \tag{2.20}$$

and

$$\begin{aligned}D(\hat{A}_0(C),\hat{A}_1(C),\hat{A}_2(C),\xi_1\hat{A}_3(C),\xi_1\hat{A}_4(C))\,|_1=1+\cos^2\theta+\hat{A}_0(C)(\tfrac{1}{2}-\tfrac{3}{2}\cos^2\theta)+\hat{A}_1(C)\sin2\theta\cos\varphi\\ +\hat{A}_2(C)\tfrac{1}{2}\sin^2\theta\cos2\varphi+\xi_1\hat{A}_3(C)\sin\theta\cos\varphi+\xi_1\hat{A}_4(C)\cos\theta\end{aligned} \tag{2.21}$$

with

$$\begin{aligned}&\hat{A}_0(C)=\hat{A}_2(C)=\frac{p_{1x}{}^2+p_{2x}{}^2}{|\vec{p}_1|^2+|\vec{p}_2|^2},\quad \hat{A}_1(C)=\frac{p_{1x}p_{1z}+p_{2x}p_{2z}}{|\vec{p}_1|^2+|\vec{p}_2|^2},\\ &\hat{A}_3(C)=\frac{|\vec{p}_1|p_{1x}+p_{2x}|\vec{p}_2|}{|\vec{p}_1|^2+|\vec{p}_2|^2},\quad \hat{A}_4(C)=\frac{|\vec{p}_1|p_{1z}+p_{2z}|\vec{p}_2|}{|\vec{p}_1|^2+|\vec{p}_2|^2} \ ,\\ &\xi_1=\frac{2\sum_i F_{1i}(x_1,x_2)x_1x_2L_i}{\sum_i F_{1i}(x_1,x_2)x_1x_2K_i} \ .\end{aligned} \tag{2.22}$$

The coefficients in the angular distribution $D(A_0(C), A_1(C), A_2(C), A_3(C), A_4(C))$ are written as

$$A_i(C)=\frac{A_i(C)(d\sigma_C/dM^2dy\,dQ_T{}^2)\,|_1+A_i(C)(d\sigma_C/dM^2dy\,dQ_T{}^2)\,|_2}{d\sigma_C/dM^2dy\,dQ_T{}^2}, \tag{2.23}$$

where

$$\frac{d\sigma_C}{dM^2dy\,dQ_T{}^2}=\int dy_j\left.\frac{d\sigma_C}{dM^2dy\,dQ_T{}^2dy_j}\right|_1+\int dy_j\left.\frac{d\sigma_C}{dM^2dy\,dQ_T{}^2dy_j}\right|_2 \tag{2.24}$$

and

$$A_i(C)\left.\frac{d\sigma_C}{dM^2dy\,dQ_T{}^2}\right|_1=\begin{cases}\int dy_j\left.\dfrac{d\sigma_C}{dM^2dy\,dQ_T{}^2dy_j}\hat{A}_i(C)\right|_1, & i=0,1,2\\ \int dy_j\left.\dfrac{d\sigma_C}{dM^2dy\,dQ_T{}^2dy_j}\xi_1\hat{A}_i(C)\right|_1, & i=3,4\end{cases} \ . \tag{2.25}$$

The corresponding formulas for case 2 can be obtained by replacing in Eqs. (2.15)–(2.17), (2.19)–(2.22), and (2.25), $F_{1i}\to F_{2i}$, $\hat{t}\leftrightarrow\hat{u}$, $U\to T$, and $\xi_1\to\xi_2$, where

$$\begin{aligned}&F_{2i}=[f_i^B(x_i)+f_{\bar{i}}^B(x_1)]f^T_{\text{gluon}}(x_2) \ ,\\ &\xi_2=\frac{2\sum_i F_{2i}(x_1,x_2)x_1x_2L_i}{\sum_i F_{2i}(x_1,x_2)x_1x_2K_i} \ .\end{aligned} \tag{2.26}$$

Finally, the total angular distribution $D(A_0,A_1,A_2,A_3,A_4)$ of Eq. (1.2) is obtained as a sum of the annihilation and the Compton contributions, where A_i's are given by

$$A_i=\frac{A_i(A)d\sigma_A/dM^2dy\,dQ_T{}^2+A_i(C)d\sigma_C/dM^2dy\,dQ_T{}^2}{d\sigma/dM^2dy\,dQ_T{}^2},\quad (i=0,1,2,3,4)\ , \tag{2.27}$$

$$d\sigma/dM^2dy\,dQ_T{}^2=d\sigma_A/dM^2dy\,dQ_T{}^2+d\sigma_C/dM^2dy\,dQ_T{}^2\ . \tag{2.28}$$

Note that a relation $A_0=A_2$ holds on account of a $\vec{p}_1\leftrightarrow\vec{p}_2$ symmetry in this model.[5]

III. NUMERICAL EVALUATION OF A_i IN pp AND $\bar{p}p$ COLLISIONS

In this section we explicitly evaluate A_i in high-energy pp and $\bar{p}p$ collisions. Integrating the angular distribution $\frac{16}{3}\pi\, dN/d\Omega_1^*=D(A_0,A_1,A_2,A_3,A_4)$, given by Eq. (1.2), over the azimuthal angle φ we get

$$\frac{dN}{d\cos\theta}=C(1+\alpha_1\cos\theta+\alpha_2\cos^2\theta)\ , \tag{3.1}$$

where

$$C=\frac{3}{8}\left[1+\frac{A_0}{2}\right],$$

$$\alpha_1=\frac{A_4}{1+\frac{1}{2}A_0},\quad \alpha_2=\frac{1-\frac{3}{2}A_0}{1+\frac{1}{2}A_o}\ . \tag{3.2}$$

And integration over θ gives

$$\frac{dN}{d\varphi}=\frac{1}{2\pi}(1+\beta_1\cos\varphi+\beta_2\cos2\varphi)\ , \tag{3.3}$$

where

$$\beta_1=\frac{3\pi}{16}A_3,\quad \beta_2=\frac{A_0}{4}=\frac{A_2}{4}\left[=\frac{1-\alpha_2}{2(\alpha_2+3)}\right]. \tag{3.4}$$

We have evaluated these coefficients in the s-channel helicity, Gottfried-Jackson and Collins-Soper frames in the c.m. system of the lepton pair (Fig. 2). The helicity frame (H) is defined by choosing the direction of a sum of the incident and the target hadron momentum as a z axis and putting the incident hadron momentum in the x-z plane in the c.m. system of the lepton pair. If one chooses the incident hadron momentum to be a z axis and puts the target momentum in the x-z plane ($P_x^T<0$), one gets the Gottfried-Jackson (GJ) frame. The Collins-Soper (CS) frame is the one where the z axis bisects the angle between $\vec{P}^B$ and $-\vec{P}^T$. (See Appendix A for variables in these frames.)

In our numerical calculations we have employed as the parton distributions those of Glück, Reya, and Owens[12], i.e., the complete scale-violating parton distributions calculated dynamically within the framework of QCD and which are valid up to very high values of M^2. We have fixed the number of flavors as $N_f=6$ and the Weinberg angle as $\sin^2\theta_W=0.23$. Thus we have used the values $M_{Z^0}=91.56$ GeV, which takes into account the increase due to loop corrections,[13] and $\Gamma_{Z^0}=2.85$ GeV, which is obtained in the Weinberg-Salam model by assuming $N_f=6$ and by taking into account the $O(\alpha_s)$ QCD corrections.[14] For the coupling constant α_s we used a formula

$$\alpha_s(Q^2)=\frac{12\pi}{(33-2N_f)}\Big/\ln(Q^2/\Lambda^2)$$

with $\Lambda=0.5$ GeV. We perform our calculations at $y=0$.

In our calculations we consider a kinematical region of high mass and small Q_T ($x_T=0.005$, 0.01, and 0.02, and also 0.1) dileptons, such that both the differential cross section $d\sigma/dM\,dy\,dQ_T{}^2$ and

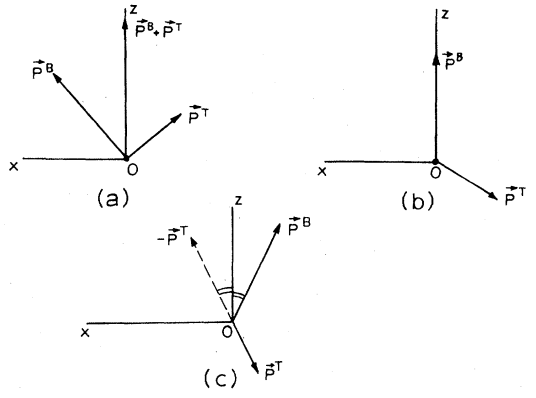

FIG. 2. Definition of reference frames in the c.m. system of the lepton pair. (a) The helicity frame. (b) The Gottfried-Jackson frame. (c) The Collins-Soper frame. $P^B=P^{\text{beam}}$, $P^T=P^{\text{target}}$.

the decay angular distributions are reasonably large to be experimentally accessible. Although the results are finite as $Q_T \to 0$, at such high energies and masses for too low value of Q_T the $O(\alpha_s)$ description of the cross section will be somehow regularized by the intrinsic transverse momentum of the partons and nonperturbative effects which start to play a role in that region.

We present in Fig. 3 the differential cross section $d\sigma/dM\,dy\,dQ_T^2$ for $p\bar{p}$ collisions at $\sqrt{s}=540$ GeV and $x_T=0.005$, as a function of M. Among the curves which are described in the figure captions we comment here only on some of them.

(i) *$\bar{p}p$ collisions at $\sqrt{s}=540$ GeV, $y=0$.* We plot α_1 in Fig. 4, α_2 in Fig. 5, and A_3 in Fig. 6 at $x_T=0.005$, 0.01, 0.02 and also in some cases at 0.1, as a function of $\sqrt{\tau}$. We also show α_1(CS) in Fig. 7 and $A_3(H)$ in Fig. 8 at $Q_T=1$, 2, 3 GeV, as functions of $r=Q_T/M$. Note that, as seen from the curves, to a good approximation the coefficients α_1(CS) and $A_3(H)$ in Figs. 7 and 8 are, in this region, functions of M only.

(ii) *pp collisions at $\sqrt{s}=800$ GeV, $y=0$.* We plot α_1 in Fig. 9, α_2 in Fig. 10, and A_3 in Fig. 11 at $x_T=0.005$, 0.01, and 0.02, as a function of $\sqrt{\tau}$.

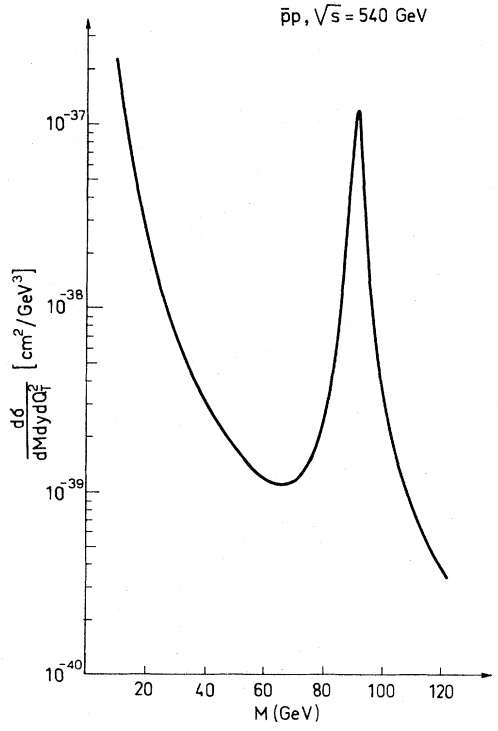

FIG. 3. The differential cross section for $\bar{p}p$ collisions at $\sqrt{s}=540$ GeV, $y=0$, and $x_T=0.005$.

We show α_1(CS) in Fig. 12 and $A_3(H)$ in Fig. 13 at $Q_T=$ 1, 2, 3 GeV, as functions of r. We notice again, by observing the curves in Figs. 12 and 13, that the coefficients α_1(CS) and $A_3(H)$ in this region are functions of M only.

For completeness, we made calculations for coefficients in pp collisions at $\sqrt{s}=63$ GeV. The result is shown in Table I. Note that the coefficients A_3 and α_1 arising from the presence of the Z^0 are

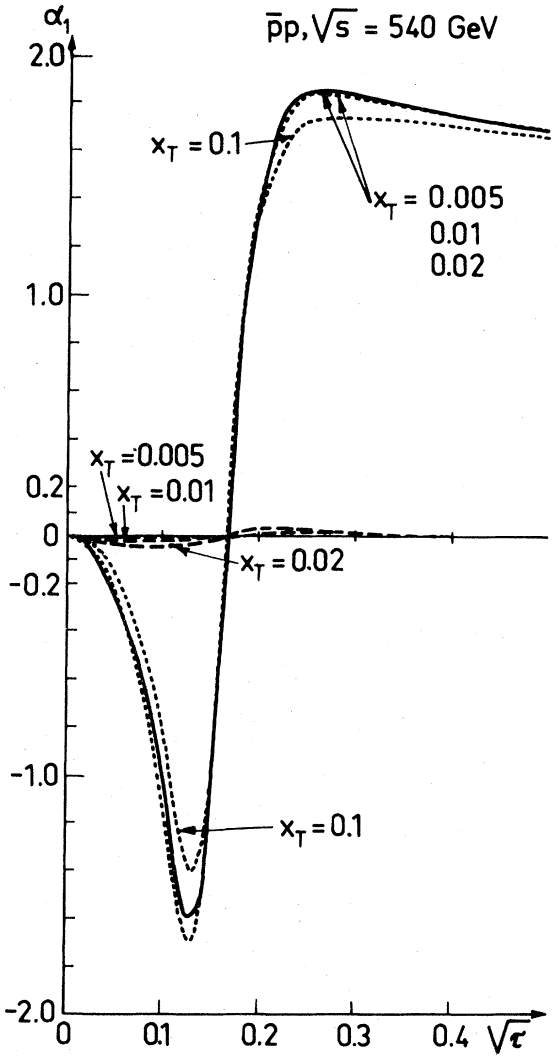

FIG. 4. Angular-distribution coefficent α_1 for $\bar{p}p$ as a function of $\sqrt{\tau}$ at $\sqrt{s}=540$ GeV, $y=0$, and $x_T=0.005$, 0.01, 0.02, and 0.1. Solid curve corresponds to Collins-Soper (CS) frame, dotted to Gottfried-Jackson (GJ), and dashed curves to helicity (H) frames. Note that in CS and GJ three curves are almost on top of each other and thus are indistinguishable.

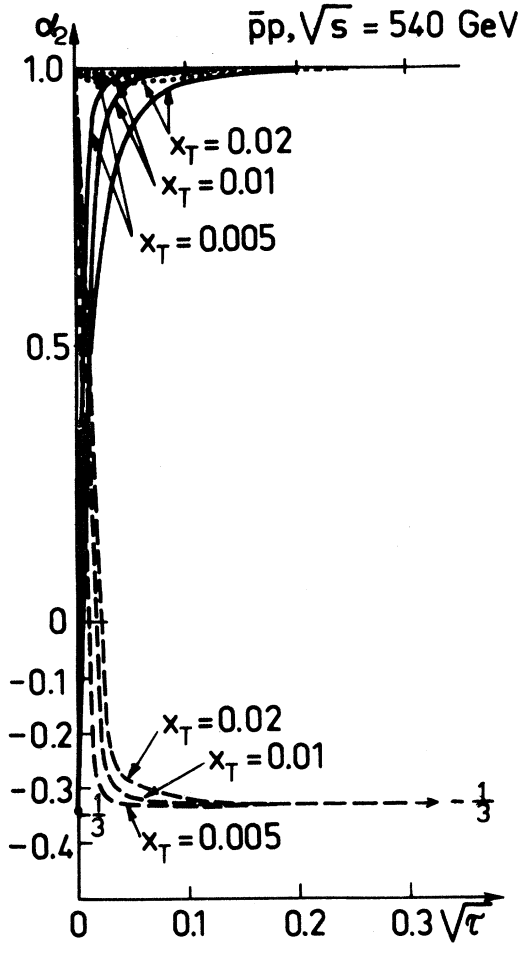

FIG. 5. Angular distribution coefficient α_2 for $\bar{p}p$ as a function of $\sqrt{\tau}$ at $\sqrt{s} = 540$ GeV, $y = 0$ and $x_T = 0.005$, 0.01, and 0.02. Solid curves are for CS, dotted for GJ, and dashed curves are for H frames.

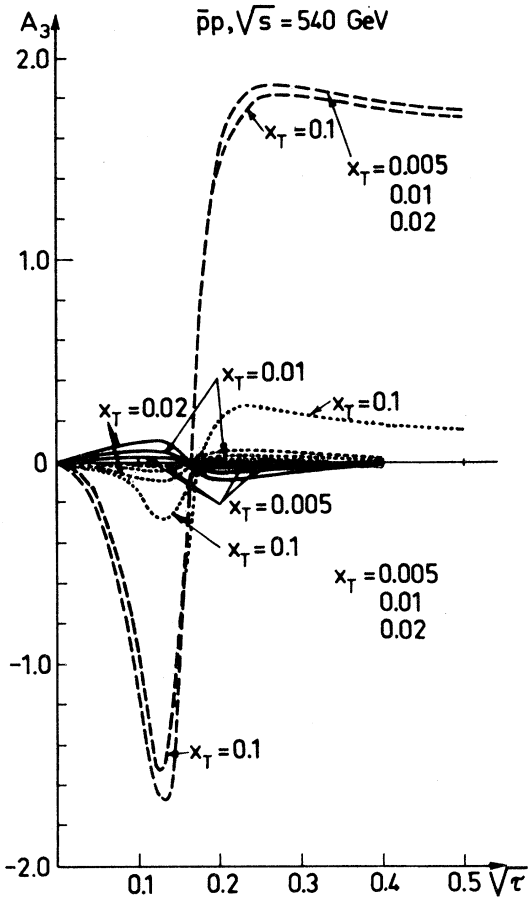

FIG. 6. Angular distribution coefficient A_3 for $\bar{p}p$ as a function of $\sqrt{\tau}$ at $\sqrt{s} = 540$ GeV, $y = 0$ and $x_T = 0.005$, 0.01, 0.02, and 0.1. Solid curves are for CS, dotted for GJ, and dashed for H frames. Note that in H, three curves are almost on top of each other.

extremely small at CERN ISR energies, as expected.

IV. CONCLUSIONS

We have calculated the angular distributions of lepton pairs decaying from γ^* and the Z^0 boson produced in hadron-hadron collisions at large M and finite Q_T. Our main conclusion is that the parity-nonconserving coefficients α_1 and A_3 clearly reflect the properties of the Z^0. Their general features are as follows: The curves of both $\alpha_1(\mathrm{GJ})$ and $\alpha_1(\mathrm{CS})$ exhibit characteristic structures, i.e., they change their sign just before the value of M reaches M_{Z^0}. The values $|\alpha_1(\mathrm{GJ})|$ and $|\alpha_1(\mathrm{CS})|$ can be rather large (see Figs. 4, 7, 9, and 12), while $|\alpha_1(H)|$ is small (see Figs. 4 and 9). On the other hand, the curves of $A_3(H)$ exhibit similar structures as those of $\alpha_1(\mathrm{GJ})$ and $\alpha_1(\mathrm{CS})$. $|A_3(H)|$ can be rather large (see Figs. 6, 8, 11, and 13), while both $|A_3(\mathrm{GJ})|$ and $|A_3(\mathrm{CS})|$ are small (see Figs. 6 and 11). Thus, measurements of $\alpha_1(\mathrm{GJ})$ and/or $\alpha_1(\mathrm{CS})$ as well as $A_3(H)$ are best suited for extracting information on the production of the Z^0 boson.

Several comments are in order.

(1) We have also calculated the coefficients, using the width $\Gamma_{Z^0} = 1.76$ GeV, which is obtained by assuming $N_f = 4$ and the mass $M_{Z^0} = 90.04$ GeV (without the loop corrections). The results, as expected, are insensitive to such a change in Γ_{Z^0} and M_{Z^0}.

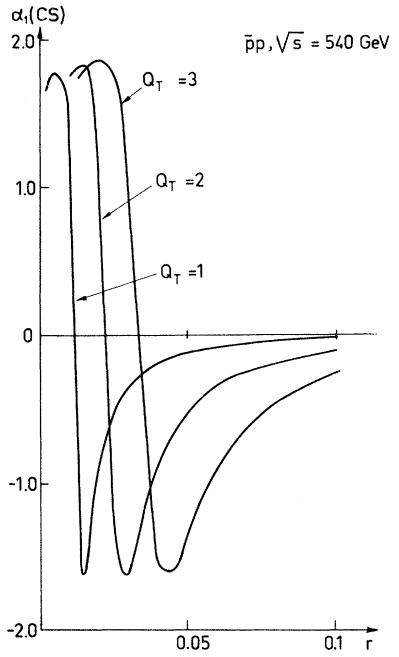

FIG. 7. Angular-distribution coefficient α_1(CS) for $\bar{p}p$ as a function of $r=Q_T/M$ at $\sqrt{s}=540$ GeV, $y=0$ and $Q_T=1$, 2, 3 GeV. Note that, as seen from these curves, to a good approximation the coefficient is a function of M only.

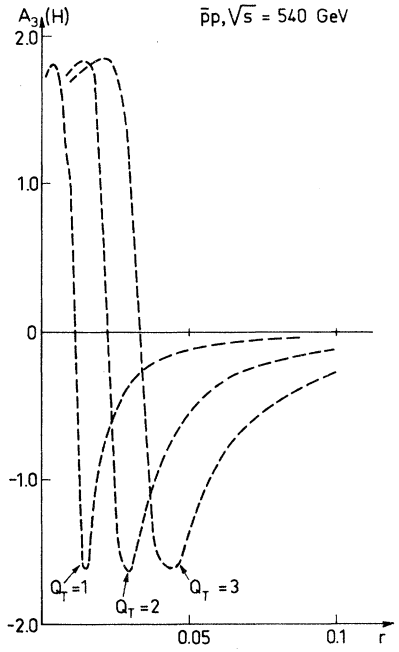

FIG. 8. Angular-distribution coefficient $A_3(H)$ for $\bar{p}p$ as a function of $r=Q_T/M$ at $\sqrt{s}=540$ GeV, $y=0$ and $Q_T=1$, 2, 3 GeV. Note that $A_3(H)\simeq\alpha_1$(CS) of Fig. 7 and that to a good approximation the coefficient is a function of M only.

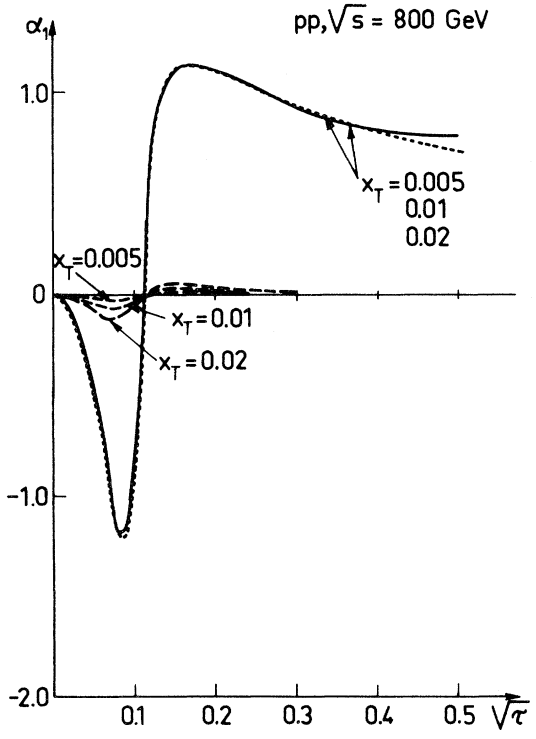

FIG. 9. Angular-distribution coefficient α_1 for pp as a function of $\sqrt{\tau}$ at $\sqrt{s}=800$ GeV, $y=0$ and $x_T=0.005$, 0.01, and 0.02. Solid curve is for CS, dotted for GJ, and dashed for H frames. Note that in CS and in GJ the three curves are almost on top of each other and thus are indistinguishable.

(2) For comparison, we have also calculated the coefficients using the completely scaling parametrization of Altarelli, Ellis, and Martinelli.[15] In the kinematical region considered, the results are quite insensitive to the choice of the parametrization.

(3) We have found that α_2 and A_1 in all of the frames almost scale in the energy range up to $\sqrt{s}=800$ GeV. It was pointed out that, in the absence of the Z^0, α_2 and A_1 scale; i.e., they are only functions of x_T and τ to the extent that the M^2 dependences of the structure functions can be neglected.[5,8] We have found that α_2 and A_1 are quite insensitive to the M^2 dependences of the parton distributions and of the propagator of the Z^0. This is due to cancellation occurring in the ratio Eq. (2.27) even if its denominator and numerator each violate scaling. Owing to the same reason the presence of the Z^0 affects α_2 and A_1 little. Thus α_2 amd A_1 are not suited for the study of the Z^0 production.

(4) On the other hand, such cancellation does not appear for α_1 and A_3 (or β_1) since ξ's appear-

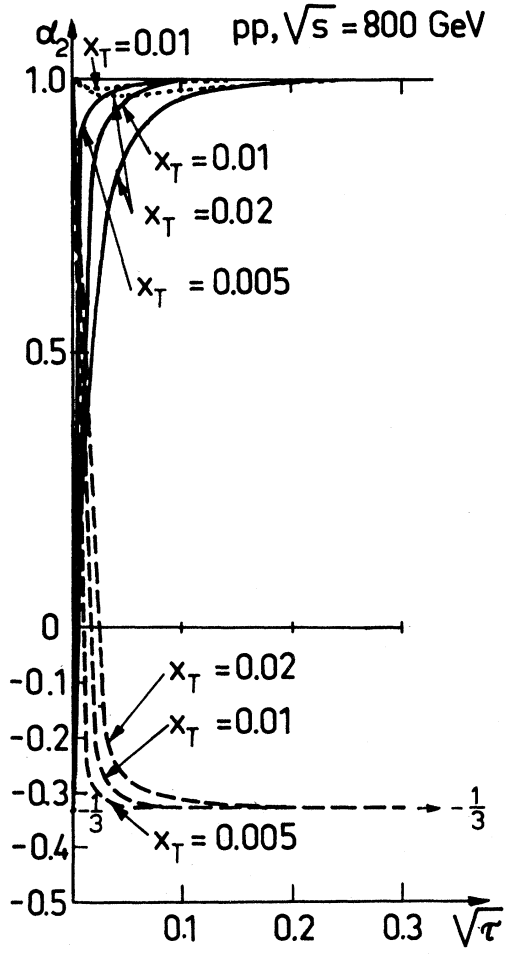

FIG. 10. Angular-distribution coefficient α_2 for pp as a function of $\sqrt{\tau}$ at $\sqrt{s}=800$ GeV, $y=0$ and $x_T=0.005$, 0.01, and 0.02. Solid curves are for CS, dotted for GJ, and dashed for H frames.

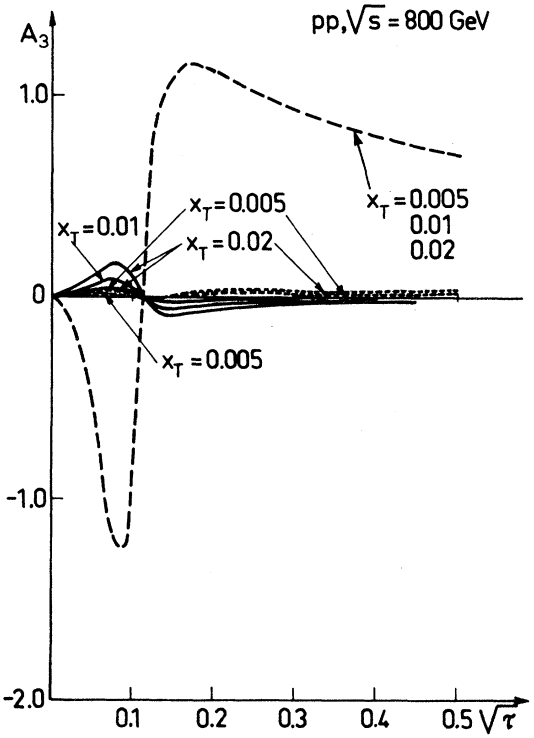

FIG. 11. Angular-distribution coefficients A_3 for pp as a function of $\sqrt{\tau}$ at $\sqrt{s}=800$ GeV, $y=0$ and $x_T=0.005$, 0.01, and 0.02. Solid curves are for CS, dotted for GJ, and dashed for H frames. Note that in H three curves are almost on top of each other.

ing in their equations, Eq. (2.9). The scaling violation is seen in α_1 and A_3.

(5) For $r=Q_T/M \ll 1$, the momenta $\vec{P}^B$ and $\vec{P}^T$ in GJ and CS frames are given by

$$\begin{aligned}
&\text{GJ: } \vec{P}^B \cong \frac{\sqrt{s}}{2}(0,0,1), \\
&\qquad \vec{P}^T \cong \frac{\sqrt{s}}{2}(-2r,0,-1), \\
&\text{CS: } \vec{P}^B \cong \frac{\sqrt{s}}{2}(-r,0,1), \\
&\qquad \vec{P}^T \cong \frac{\sqrt{s}}{2}(-r,0,-1).
\end{aligned} \tag{4.1}$$

Hence for $r \ll 1$, one has

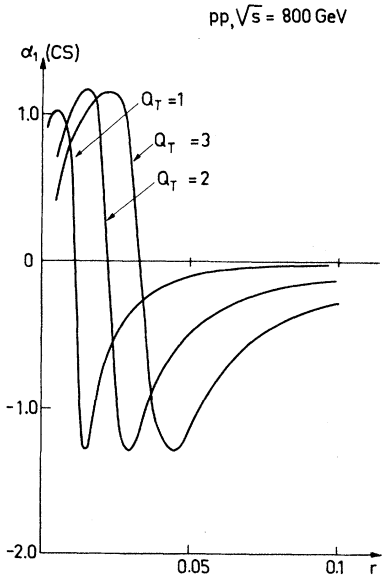

FIG. 12. Angular-distribution coefficient α_1(CS) for pp as a function of $r=Q_T/M$ at $\sqrt{s}=800$ GeV, $y=0$ and $Q_T=1$, 2, 3 GeV. Note that, as seen from these curves, to a good approximation the coefficient α_1(CS) is a function of M only.

TABLE I. Values of the angular correlation coefficients α_1, α_2, and A_3 for $pp \to$ lepton pair at $y=0$, $x_T=0.0635$ ($Q_T=2$ GeV) and $\sqrt{s}=63$ GeV and at different values of $\sqrt{\tau}=M/\sqrt{s}$.

$\sqrt{\tau}$	0.1	0.2	0.3	0.4
GJ frame				
α_1	−0.007	−0.026	−0.054	−0.088
α_2	0.83	0.92	0.95	0.97
A_3	0.001	0.016	0.017	0.024
H frame				
α_1	−0.002	−0.002	−0.005	0.003
α_2	−0.16	−0.28	−0.310	−0.32
A_3	−0.008	−0.026	−0.050	−0.079

$$A_i(\mathrm{GJ}) \cong A_i(\mathrm{CS}) \ . \tag{4.2}$$

This feature can be seen in Figs. 4 and 9.

(6) One can obtain the angular distribution for the Drell-Yan process via γ^* and Z^0 from that for the annihilation process by taking the limit $Q_T \to 0$. Using Eqs. (2.12), (2.13), and (1.2) together with Eqs. (A1) and (A2), we obtain in the GJ frame

$$D = \frac{16\pi}{3}\frac{dN}{d\Omega_1^*} = \begin{cases} 1+\cos^2\theta+\xi\cos\theta, & \text{for } \bar{p}p \text{ collisions} \\ 1+\cos^2\theta, & \text{for } pp \text{ collisions} \end{cases} \tag{4.3}$$

The presence of the term containing ξ in $\bar{p}p$ collisions reflects the parity-nonconserving effect of the Z^0 boson. For $M \ll M_{Z^0}$ we have $\xi \to 0$, hence we obtain $D \to 1+\cos^2\theta$, consistent with the well-known Drell-Yan distribution mentioned in Sec. I.

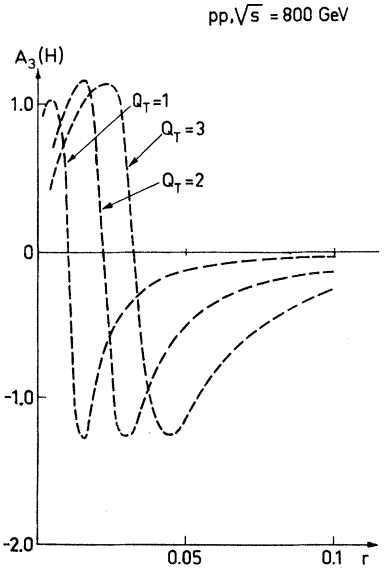

FIG. 13. Angular-distribution coefficient $A_3(H)$ for pp as a function of $r=Q_T/M$ at $\sqrt{s}=800$ GeV, $y=0$ and $Q_T=1$, 2, 3 GeV. Note that $A_3(H) \simeq \alpha_1(\mathrm{CS})$ of Fig. 12 and that to a good approximation the coefficient is a function of M only.

(7) Our calculations based on the first-order QCD perturbation are certainly more reliable for the $\bar{p}p$ case. The reasons are as follows: First the valence quark distributions are much better known than the sea and gluon distributions. Second, in the $\bar{p}p$ case, the $O(\alpha_s)$ annihilation contribution is large and hence the $O(\alpha_s^2)$ bremsstrahlung contribution can be safely neglected compared to the annihilation one. On the other hand, in pp collisions, the $O(\alpha_s^2)$ bremsstrahlung term, in which both valence quarks take part in the scattering, gives a substantial contribution under certain kinematical condition[16,17] compared to the annihilation one. Our calculations, in which this contribution is completely neglected, are thus less reliable for pp collisions. The issue of such $O(\alpha_s^2)$ bremsstrahlung contribution in the lepton angular distributions in pp collisions will no doubt deserve further study.

ACKNOWLEDGMENT

It is our pleasure to thank J. Lindfors for several useful discussions and reading the manuscript.

APPENDIX A

Let us list kinematical variables used in this paper in terms of scaling variables.[5]

Initial momenta of constituents are given by

$p_1=x_1P^B$, $p_2=x_2P^T$ for annihilation ,

$p_1=x_2P^T$, $k=x_1P^B$ for Compton scattering, case 1 ,

$p_1=x_1P^B$, $k=x_2P^T$ for Compton scattering, case 2 .

In the lepton-pair rest system momenta of the incident and the target hadrons are given as follows. Helicity frame:

$$\vec{P}^B=\frac{\sqrt{s}}{2}\frac{1}{(\bar{x}_T^2\cosh^2 y-4\tau)^{1/2}}\left[x_T,0,\frac{\bar{x}_T^2e^{-2y}+x_T^2-4\tau}{4\sqrt{\tau}}\right],$$

$$\vec{P}^T=\frac{\sqrt{s}}{2}\frac{1}{(\bar{x}_T^2\cosh^2 y-4\tau)^{1/2}}\left[-x_T,0,\frac{\bar{x}_T^2e^{2y}+x_T^2-4\tau}{4\sqrt{\tau}}\right], \tag{A1}$$

$x_T=2Q_T/\sqrt{s}$, $\tau=M^2/s$, $\bar{x}_T=\sqrt{x_T^2+4\tau}$.

Gottfried-Jackson frame:

$$\vec{P}^B=\frac{s\bar{x}_T}{4M}e^{-y}(0,0,1),\quad \vec{P}^T=\frac{s\bar{x}_T}{4M}e^{y}\left[-4\sqrt{\tau}x_T/\bar{x}_T^2,0,\frac{x_T^2-4\tau}{\bar{x}_T^2}\right]; \tag{A2}$$

Collins-Soper frame:

$$\vec{P}^B=\frac{s}{4M}e^{-y}(x_T,0,2\sqrt{\tau}),\quad \vec{P}^T=\frac{s}{4M}e^{y}(-x_T,0,-2\sqrt{\tau}) . \tag{A3}$$

Invariant variables are written as

$$\hat{s}=x_1x_2s,\quad \hat{t}=s(\tau-x_1x_2+V)/2,\quad \hat{u}=s(\tau-x_1x_2-V)/2,\quad V=[(x_1x_2-\tau)^2-x_1x_2x_T^2]^{1/2} .$$

Finally, relations of scaling variables x_1, x_2, and y_j are given by

$$(x_1-\tfrac{1}{2}\bar{x}_Te^{y})(x_2-\tfrac{1}{2}\bar{x}_Te^{-y})=x_T^2/4,\quad x_1=(\bar{x}_Te^{y}+x_Te^{y_j})/2,\quad x_2=(\bar{x}_Te^{-y}+x_Te^{-y_j})/2 . \tag{A4}$$

[1]Y. Nambu, in *Proceedings of the 19th International Conference on High Energy Physics, Tokyo, 1978,* edited by S. Homma, M. Kawaguchi, and H. Miyazawa (Phys. Soc. of Japan, Tokyo, 1979).

[2]I. Hinchliffe and C. H. Llewellyn Smith, Phys. Lett. 66B, 281 (1977); Nucl. Phys. B128, 93 (1977); J. Kogut and J. Shigemitsu, *ibid.* B129, 461 (1977); L. B. Okun and M. B. Voloshin, *ibid.* B120, 459 (1977); R. Plamer, E. Paschos, N. Samios, and L. L. Wang, Phys. Rev. D 14, 118 (1976); R. F. Peierls, T. L. Trueman, and L. L. Wang, *ibid.* 16, 1397 (1977); C. Quigg, Rev. Mod. Phys. 49, 297 (1977); T. M. Yan, in *Proceedings of the VIII International Symposium on Multiparticle Dynamics, Kayserberg, France, 1977* (Centre de Recherches Nucléaires, Strasbourg, France, 1977), p. C-21; F. Halzen, Phys. Rev. D 15, 1929 (1977); F. Halzen and D. M. Scott, Phys. Lett. 78B, 318 (1978); M. Perottet, Ann. Phys. (N.Y.) 115, 107 (1978); M. Chaichian and M. Hayashi, Phys. Lett. 81B, 53 (1979); M. Chaichian, O. Dumbrajs, and M. Hayashi, Phys. Rev. D 20, 2873 (1979); F. E. Paige, talk at Topical Conference on the Production of New Particles in Super High Energy Collisions, Madison, Wisconsin, 1979, BNL Report No. 27066 (unpublished); B. Humpert and W. L. van Neerven, Phys. Lett. 93B, 456 (1980); P. Aurenche and J. Lindfors, *ibid.* 96B, 171 (1980); Nucl. Phys. B185, 274 (1981); B185, 301 (1981).

[3]V. Vasavada, Phys. Rev. D 16, 146 (1977); E. L. Berger, J. T. Donohue, and S. Wolfram, *ibid* 17, 858 (1978).

[4]J. C. Collins and D. E. Soper, Phys. Rev. D 16, 2219 (1977).

[5]K. Kajantie, J. Lindfors, and R. Raitio, Phys. Lett. 74B, 384 (1978); Nucl. Phys. B144, 422 (1978).

[6]M. Noman and S. D. Rindam, Phys. Rev. D 19, 207 (1979).

[7]J. Cleymans and M. Kuroda, Phys. Lett. 80B, 385 (1979); Nucl. Phys. B155, 480 (1979).

[8]J. C. Collins, Phys. Rev. Lett. 42, 291 (1979).

[9]J. Lindfors, Phys. Scr. 20, 19 (1979); R. L. Thews, Phys. Rev. Lett. 43, 987 (1979); *ibid.* 43, 1968(E) (1979).

[10]S. D. Drell and T. M. Yan, Phys. Rev. D 16, 2219 (1977).
[11]D. Politzer, Nucl. Phys. B129, 301 (1977); G. Altarelli, G. Parisi, and R. Petronzio, Phys. Lett. 76B, 351 (1978); 76B, 356 (1978).
[12]M. Glück and E. Reya, Nucl. Phys. B130, 91 (1977); J. E. Owens and E. Reya, Phys. Rev. D 17, 3003 (1978).
[13]M. Veltman, Phys. Lett. 91B, 95 (1980).
[14]D. Alberto, W. J. Marciano, D. Wyler, and Z. Parsa, Nucl. Phys. B166, 460 (1980).
[15]G. Altarelli, R. K. Ellis, and G. Martinelli, Nucl. Phys. B157, 461 (1979).
[16]M. Chaichian, M. Hayashi, and T. Honkaranta, Nucl. Phys. B157, 493 (1980).
[17]A. Contogouris, R. Gaskell, and L. Marleau, Phys. Rev. D 22, 1109 (1980); A. Contogouris, J. Kripfganz, L. Marleau, and S. Papadopoulos, McGill University Report No. 80-355, 1980 (unpublished).